Beamforming Design for NOMA-Assisted Symbiotic Backscatter

Fatemeh Rezaei[†], Diluka Galappaththige[†], Chintha Tellambura[†], and Amine Maaref[‡]
[†]Department of Electrical and Computer Engineering, University of Alberta, Edmonton, AB, T6G 1H9, Canada
[‡]Huawei Canada, 303 Terry Fox Drive, Suite 400, Ottawa, Ontario K2K 3J1
Email: {rezaeidi, diluka.lg, ct4}@ualberta.ca, amine.maaref@huawei.com

***Abstract*—Optimal beamforming design is developed for a non-orthogonal multiple access (NOMA)-aided symbiotic radio (SR) system where a base station (BS) simultaneously serves multiple NOMA users and a secondary ambient tag. The nearest user of the tag decodes its own data and the tag data using the successive interference cancellation (SIC) technique. We design optimal transmit beamforming and power allocation at the BS to maximize the weighted sum rate of NOMA users and the tag, under the minimum rate requirements while satisfying the tag's minimum energy requirement. Because the problem is non-convex, we propose algorithms using alternative optimization and fractional programming techniques. Our results reveal that significant performance gains can be achieved while keeping the tag design intact. For example, the proposed beamforming can increase harvested power and data rate by $2.16 \times 10^3\,\%$ and $314.5\,\%$ compared to random beamforming.**

I. Introduction

Symbiotic radio (SR), as a strategy to promote win-win growth of spectral efficiency (SE) and energy efficiency (EE), enables primary and secondary networks to cooperate in bandwidth, power, and other resource sharing [1]. For example, smart home sensors (tags) in an Internet-of-Things (IoT) network can live together with a cellular network (Fig. 1). Both positive (beneficial) and negative (harmful) associations are therefore included. Thus, mutualistic or competitive symbiotic relationships can exist. If primary and secondary data rates are R_p and R_s, we can classify SR as commensal SR (CSR) or parasitic SR (PSR) [1]. In CSR, $R_s \ll R_p$ and the secondary signal is treated as a multi-path component. In PSR, $R_p = R_s$ and secondary signals directly interfere with primary signals. Multi-objective optimization is thus necessary to simultaneously improve the performance of both networks [1].

Backscatter networks are a natural candidate for symbiosis. Backscatter tags passively reflect a radio frequency (RF) signal to communicate their data while harvesting energy from the same RF signal [2], [3]. Hence, tags eschew active RF components, resulting in ultra-low-power consumption, low complexity, and low cost, which are hugely positive benefits. Energy harvesting (EH) can power tags, which save batteries and associated costs. We focus on ambient backscatter communication (AmBC), where the RF signal is an ambient one transmitted by legacy (primary) sources, such as cellular base stations (BSs), Wi-Fi access points, etc. [2], [3]. Therefore, AmBC has no new spectrum allocations, no licensing and regulatory hurdles, and no need for dedicated RF emitters. The symbiosis of AmBC and conventional primary systems should yield the best of both worlds. Another advantage is that only minor modifications to the primary system are made. For instance, the primary BS can be modified to support both networks and end their interactions. Likewise, primary users can decode data from both networks by employing successive interference cancellation (SIC) decoding techniques [4].

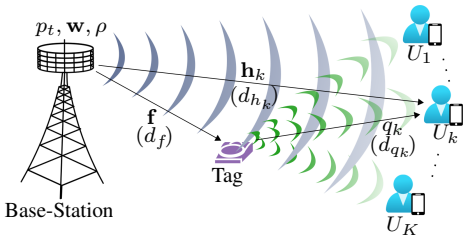

Fig. 1: Multiple users supported with a single tag.

As the primary symbiont, we choose a non-orthogonal multiple access (NOMA) network (Fig. 1). NOMA allows users to access the same spectrum resource simultaneously [5]. Thus, it is natural to integrate NOMA with AmBC to improve SE and EE for large-scale passive IoT networks [6]. For this reason, research into such integrated systems has surged recently. In particular, in [7], a single-antenna BS serves two NOMA primary users and a tag in a CSR setup. The symbiosis benefit to the primary system (rate increase) is maximized by jointly optimizing the power allocation factor, ρ, and reflection coefficient at the tag, α. For the same system setup, [8] investigates the symbiosis benefits to the primary system in terms of EE. Reference [9] also investigates the primary system's EE by extending [7] to a multi-cell scenario. Symbiotic NOMA-assisted vehicular network with tags is also investigated in [10] and [11] where roadside units relay information to vehicles through NOMA, and tags assist this task in a CSR/PSR setup. The primary system's EE which is subjected to rate constraint [10] and the minimum achievable rate of the vehicles [11] are then maximized.

Unlike [7]–[10], which maximize the symbiosis benefits to the primary network neglecting the tag's performance, the works [6], [12] study the symbiosis benefits/harms to both the tag and the primary users. In particular, [12] considers two NOMA users and maximizes the symbiosis benefit to the tag (rate) while preserving the primary outage by jointly optimizing α and ρ. And [6] maximizes the symbiosis benefits for a RIS-assisted NOMA system in terms of the overall EE by jointly optimizing the phase shifts at the RIS and ρ.

These works, however, do not evaluate how beamforming

designs add to symbiosis. Thus, the full benefits and harms of symbiosis should be further investigated. In addition, except for [12], no other study has considered the EH requirement of the tag. Furthermore, most relevant works [6]–[8], [12] consider the basic two-user NOMA setup.

Motivation and Our Contributions: In the paper, we investigate several fundamental questions about symbiotic NOMA (primary) +AmBC (secondary) networks (Fig. 1). These are (i) How can the BS design be improved to maximize the benefits or minimize the harms for both networks? and (ii) How to ensure tag activation with enough energy? To answer these important questions, we consider a PSR network of $K(\geq 2)$ users and one tag (Fig. 1). The BS uses a common beamformer to shape its RF signal to serve users and tag to achieve symbiosis. The tag harvests energy from the BS signal and reflects it to send data to the users. The nearest user decodes the tag data via SIC. Thus, the main problems are to design an optimal transmit beamformer, $\mathbf{w}$, and power allocation factor, ρ, at the BS with rate and energy constraints.

The main contributions of this paper are as follows: (i) To achieve symbiosis, we maximize the weighted sum-rate (WSR) of NOMA users and the tag. The problem requires joint optimization of $\mathbf{w}$ and ρ. Due to intricately coupled variables in the signal-to-interference-plus-noise ratio (SINR)/signal-to-noise ratio (SNR), this problem has a non-convex objective and constraints. Thus, common convex algorithms are not able to handle it. Hence, we split it into two sub-problems, namely $\mathbf{P}_{\mathrm{w}}$ and $\mathbf{P}_{\rho}$. We then employ alternating optimization (AO) and solve these iteratively using the fractional programming (FP) technique, (ii) The proposed algorithms improve symbiotic performance gains while keeping the tag design intact. Thus, symbiotic gains and passive tags can help realize passive IoT networks, (iii) Finally, we present numerical examples to evaluate the symbiotic gains through the proposed solutions.

II. System Model and Preliminaries

A. System and Channel Models

Fig. 1 shows an SR network that comprises a BS, as the primary transmitter, equipped with $M \geq 1$ antennas, K primary single-antenna users denoted by $U_k, k \in \mathcal{K} \triangleq \{1, \ldots, K\}$, and a single-antenna tag, which are all located nearby, e.g., within a room. The BS serves the primary NOMA users. Without loss of generality, we assume that the nearest user, U_1, to the tag decodes the tag's data. However, U_1 may not necessarily have the strongest channel gain among the NOMA users. The tag is powered by EH. The tag communicates by reflecting the incident RF signal. Hence, the BS transmits its data to the users via transmit beamforming, simultaneously enabling the tag to send its data, which is decoded by U_1.

We consider block flat-fading channel models. During each fading block, channel response vectors between U_k and the BS is given as $\mathbf{h}_k \in \mathbb{C}^{M\times 1}$. Moreover, $\mathbf{f} \in \mathbb{C}^{M\times 1}$ is the forward-link channel vector between the tag and the BS, and $q_k \in \mathbb{C}$ is the channel between the tag and U_k. A unified representation of all five channels is given as

$$\mathbf{a} = \zeta_{\mathbf{a}}^{1/2}\tilde{\mathbf{a}}, \quad \text{for} \quad \mathbf{a} \in \{\mathbf{h}_k, \mathbf{f}, q_k\} \quad \text{and} \quad k \in \mathcal{K}, \tag{1}$$

where $\zeta_{\mathbf{a}}$ accounts for the large-scale path-loss and shadowing. Moreover, $\tilde{\mathbf{a}} \sim \mathcal{CN}(\mathbf{0}, \mathbf{I}_M)$ captures Rayleigh fading.

The CSI acquisition of the SR system can be performed via pilot transmission. In particular, by carefully designing a set of orthogonal pilot sequences, the direct user channel and cascaded channels, i.e., the users-tag-BS channel, can be estimated during the channel training period, as proposed in [13]. For the sake of brevity, we omit the details and refer interested readers to [13]. We thus assume that perfect CSI is available.

B. Data Transmission and EH at the tag

The tag exploits power switching protocol to perform EH and data transmission, simultaneously, where each operation captures a fraction of the incident RF power p_a [2]. It thus reflects αp_a and harvests $p_l = (1-\alpha)p_a$. The tag symbol $c(n)$ ($\mathbb{E}\{|c(n)|^2\} = 1$), is selected from a $\bar{M}$-ary constant-envelope modulation. The tag modulation process is described in [2].

We assume a linear EH model for its tractability. In this model, the harvested power is given by $p_h = \eta_b p_l$, where $\eta_b \in (0, 1]$ is the power conversion efficiency. The tag must harvest more than a minimum threshold (p_b), around $-20\,\mathrm{dBm}$ [2], to maintain its operation, i.e., $p_h \geq p_b$.

C. Transmission Model

The BS transmits signal $s_k(n)$ to U_k ($k \in \mathcal{K}$) at the n-th time slot, where $E\{|s_k(n)|^2\} = 1$, with transmission power $\rho_k p_t$, where p_t is the total BS power and $\rho_k \in (0, 1)$ is the power allocation coefficient for U_k. With K-user NOMA, $s_k(n)$ are superimposed as $x(n) = \sum_{k\in\mathcal{K}} \sqrt{\rho_k p_t} s_k(n)$, where the set of power coefficients $\{\rho_k\}$ satisfies $\sum_{k\in\mathcal{K}} \rho_k = 1$. Furthermore, the different data signals are mutually uncorrelated; $\mathbb{E}\{s_k(n)s_i^*(n)\} = \delta(k-i)$, where $k, i \in \mathcal{K}$ [14]. Therefore, $\mathbb{E}\{|x(n)|^2\} = \sum_{k\in\mathcal{K}} \rho_k p_t = p_t$.

The tag harvests energy from $x(n)$ and also reflects $x(n)$ its binary signal, $c(n)$, $\mathbb{E}\{|c(n)|^2\} = 1$. The users thus receive the tag reflection and $x(n)$. Assuming negligible propagation delay differences [8], the received signal at U_k is given as

$$y_k(n) = \mathbf{h}_k^{\mathrm{H}}\mathbf{w}x(n) + \sqrt{\alpha}\mathbf{g}_k^{\mathrm{H}}\mathbf{w}x(n)c(n) + n_k(n), \tag{2}$$

where the first term is the direct-link signal and the second term is the backscatter-link signal. Besides, $\mathbf{g}_k = \mathbf{f}q_k$ is the backscatter link between U_k and the BS. Moreover, $\mathbf{w} \in \mathbb{C}^{M\times 1}(\|\mathbf{w}\|^2 = 1)$, denotes the BS beamforming vector. Furthermore, $n_k \sim \mathcal{CN}(0, \sigma^2)$ denotes the additive white Gaussian noise (AWGN) at U_k. We assume that the primary signal $s_k(n), k \in \mathcal{K}$, and the tag signal $c(n)$ are standard circular symmetric complex Gaussian variables, $\mathcal{CN}(0, 1)$ [1].

Without loss of generality, we assume that U_1, which is located nearest to the tag, decodes the tag's signal. Hence, to

guarantee successful decoding of the tag's signal, we assume the users are ordered based on the effective channel gains:

$$|\mathbf{h}_1^{\mathrm{H}}\mathbf{w}|^2 \geq |\mathbf{h}_2^{\mathrm{H}}\mathbf{w}|^2 \geq \ldots \geq |\mathbf{h}_K^{\mathrm{H}}\mathbf{w}|^2. \tag{3}$$

Thus, higher power is allocated to the user with lower effective channel strength, i.e., $\rho_1 \leq \cdots \leq \rho_K$ where U_k applies SIC to decode $s_k(n)$. More precisely, U_k decodes $s_k(n)$ of the users with higher powers ($\forall i > k$) , and then subtracts them from the received signal $y_k(n)$ (2). Moreover, U_k treats the signals of the other users with higher effective channel strength ($\forall i < k$), and the tag's signal as interference[1]. User U_1 performs SIC to decode $s_1(n)$ and other users' signals and subtracts them from the received signal when decoding the tag's signal.

Mathematically, the condition that U_k can perform SIC and decode the data intended for the users with lower effective channel strength, can be written as [14]

$$\mathbb{E}\{\log_2(1+\gamma_k^i)\} \geq \mathbb{E}\{\log_2(1+\gamma_i^i)\}, \quad \forall i > k. \tag{4}$$

In (4), γ_k^i is the effective SINR of U_i at U_k, when U_k decodes the signal intended for U_i. We must note that allocating higher powers to users with lower effective channel strength also yields a non-trivial data rate for them [14].

Thus, the received signal at U_k (2) after an perfect SIC process can be written as

$$\bar{y}_k(n) = \underbrace{\mathbf{h}_k^{\mathrm{H}}\mathbf{w}\sqrt{\rho_k p_t}s_k(n)}_{\text{Desired signal}} + \underbrace{\mathbf{h}_k^{\mathrm{H}}\mathbf{w}\sum\nolimits_{i=1}^{k-1}\sqrt{\rho_j p_t}s_j(n)}_{\text{Interference after SIC}} + \underbrace{\sqrt{\alpha}\mathbf{g}_k^{\mathrm{H}}\mathbf{w}x(n)c(n)}_{\text{Interference from the tag}} + n_k(n). \tag{5}$$

D. Achievable Rate

This section derives the user and the tag rates. Using the rate inequality in (4), the rate of U_k is computed as

$$\mathcal{R}_k = \log_2(1+\gamma_k), \tag{6}$$

where $\gamma_k \triangleq \min(\gamma_k^k, \gamma_i^k), \forall i < k$ to guarantee that U_i ($\forall i < k$) can perform SIC and decode the data of U_k. Following the same principle as (5), for the received signal at the typical user $U_i, \forall i < k$, by considering the first term in (5) as the desired signal and the remaining terms as an effective noise, the SINR of U_k at U_i, γ_i^k, can be derived as[2]

$$\gamma_i^k = \frac{\rho_k p_t |\mathbf{h}_i^{\mathrm{H}}\mathbf{w}|^2}{|\mathbf{h}_i^{\mathrm{H}}\mathbf{w}|^2 p_t \sum_{j=1}^{k-1}\rho_j + \alpha p_t |\mathbf{g}_i^{\mathrm{H}}\mathbf{w}|^2 + \sigma^2}. \tag{7}$$

On the other hand, U_1 decodes the tag's signal by performing SIC and subtracting its decoded signal and other users' signals. Thus, the rate of the tag after perfect SIC is given as

$$R_0 = \mathbb{E}_x\left\{\log_2(1+\gamma_0^b)\right\}, \quad \text{and} \quad \gamma_0^b = \frac{\alpha|\mathbf{g}_1^{\mathrm{H}}\mathbf{w}|^2|x(n)|^2}{\sigma^2}. \tag{8}$$

[1]Direct-link signal is typically stronger than the backscatter-link signal [1].

[2]The distribution of $c(n)s_k(n)$ is approximated as circular symmetric complex Gaussian, yielding a lower bound of the achieved rate [1].

In (8), γ_0^b is the received SINR of the tag at U_1. By taking the average over $x(n)$ in (8), the rate of the tag is given as

$$R_0 = -e^{1/\gamma_0'}\mathrm{E}_i\left(-1/\gamma_0'\right)\log_2(e), \tag{9}$$

where γ_0' is the average received SINR of the backscatter link and is given as $\gamma_0' = \alpha p_t |q_1|^2 |\mathbf{f}_1^{\mathrm{H}}\mathbf{w}|^2/\sigma^2$. Additionally, $\mathrm{E}_i(x) = \int_{-\infty}^{x} u^{-1}e^u du$ and it is worth noting that, $-e^{1/\gamma_0'}\mathrm{E}_i(-1/\gamma_0')$ is monotonically increasing and concave function of γ_0' [1].

As per Section II-B, the tag needs to harvest enough power. Therefore, the linear EH model imposes the constraint

$$\eta_b(1-\alpha)p_a \geq p_b, \quad \text{and} \quad p_a = |\mathbf{f}^{\mathrm{H}}\mathbf{w}|^2 p_t. \tag{10}$$

III. Optimization Problem Formulation

Herein, the optimization variables are BS beamforming vector, $\mathbf{w}$, and NOMA power allocation factors, $\boldsymbol{\rho} = [\rho_1, \ldots, \rho_K]$. We maximize the network WSR. We ensure that all the $K+1$ nodes achieve a minimum rate and the tag meets the minimum operating energy threshold. To this end, we formulate the WSR maximization (WSRMax) problem, $\mathbf{P}$. WSRMax provides a framework to integrate the rate constraints, the tag EH constraint, and the BS power constraint in order to simultaneously satisfy the demands of both networks and improve their performance symbiotically. However, the power allocation entangles the beamforming design due to the rate constraints, complicating the problem. This problem addresses two main goals for realizing passive IoT. First, symbiotic gains are achieved in terms of the achievable rate. Second, connectivity is established in large-scale passive IoT networks.

The WSRMax problem can be formulated as

$$\begin{aligned}
\mathbf{P}: \underset{\mathbf{w},\boldsymbol{\rho}}{\text{maximize}} \; & \sum\nolimits_{k\in\mathcal{K}_0} a_k R_k, \\
\text{s.t.} \; & C_1: R_k \geq R_k^{\mathrm{th}}, \quad \text{for} \quad k \in \mathcal{K}_0, \\
& C_2: \rho_1 \leq \cdots \leq \rho_K, \text{ and } \sum\nolimits_{k\in\mathcal{K}} \rho_k = 1, \\
& C_3: \eta_b(1-\alpha)|\mathbf{f}^{\mathrm{H}}\mathbf{w}|^2 p_t \geq p_b, \\
& C_4: \|\mathbf{w}\|^2 = 1, \\
& C_5: |\mathbf{h}_1^{\mathrm{H}}\mathbf{w}|^2 \geq \ldots \geq |\mathbf{h}_K^{\mathrm{H}}\mathbf{w}|^2,
\end{aligned} \tag{11}$$

where $a_k \in [0,1]$ for $k \in \mathcal{K}_0 \triangleq \{0,1,\ldots,K\}$ is the weight factor and $\sum_{k\in\mathcal{K}_0} a_k = 1$. Note that C_1 constraint guarantees the required rate for $U_k, k \in \mathcal{K}$, and the tag, in which $R_k^{\mathrm{th}}, k \in \mathcal{K}_0$ denotes the minimal rate requirement of respective users and the tag, and R_k, $k \in \mathcal{K}_0$ is given in (6) and (8), respectively. Besides, C_2 is the transmit power allocation constraint at the BS, C_3 is the minimum tag power requirement, and C_4 is the normalization constraint for the BS transmit beamforming. We assume a fixed reflection coefficient at the tag. This assumption is consistent with passive tags [4].

We note that $\mathbf{P}$ is not convex since the objective function and the corresponding constraints are not convex functions in either of the optimization variables, i.e., $\mathbf{w}$, and $\boldsymbol{\rho}$. Hence, we first transform the problem into convex form and use the AO technique to solve $\mathbf{P}$. In what follows, we propose solutions to the above optimization problem.

IV. Proposed Solutions

First, we replace the rate of the tag, given in (8), with its lower bound for mathematical simplicity and to solve the proposed optimization problems as [15]

$$R_0 \geq R_0^{\mathrm{lb}} \triangleq \log_2\left(1+\left[\mathbb{E}\left\{1/\gamma_0^b\right\}\right]^{-1}\right) \overset{(a)}{=} \log_2(1+\gamma_0), \quad (12)$$

where $\gamma_0 = \gamma_0'/2$ (9), and (a) is obtained by using $\mathbb{E}\{1/\gamma_0^b\} = 1/\mathbb{E}\{\gamma_0^b\} + \sigma^2_{\gamma_0^b}/[\mathbb{E}\{\gamma_0^b\}]^3$, in which γ_0^b is given in (8).

Because of the non-convex objective and constraints, $\mathbf{P}$ is not amenable to conventional convex optimization methods. Besides, the joint optimization of $\mathbf{w}$ and $\boldsymbol{\rho}$ is complicated. Hence, we seek a simpler solution for $\mathbf{P}$ by decoupling the optimization variables, $\mathbf{w}$ and $\boldsymbol{\rho}$, to reduce $\mathbf{P}$ into two sub-problems. Thereby, for a given power allocation factor $\boldsymbol{\rho}$, $\mathbf{P}$ is reduced to a transmit beamforming optimization problem as

$$\begin{aligned}\mathbf{P}_{\mathrm{w}}: \underset{\mathbf{w}}{\text{maximize}} \;& \sum\nolimits_{k\in\mathcal{K}_0} a_k \log_2(1+\gamma_k), \\ \text{s.t.} \;& C_1: \gamma_k \geq \gamma_k^{\mathrm{th}}, \quad \text{for} \quad k \in \mathcal{K}_0, \\ & C_3 - C_5, \end{aligned} \quad (13)$$

where $\gamma_k^{\mathrm{th}} = 2^{R_k^{\mathrm{th}}} - 1$ and the rate requirement constraint C_1 is equivalently converted to SINR constraint, since R_k is a non-decreasing function of its argument. Similarly, for a given $\mathbf{w}$, $\mathbf{P}$ becomes a power allocation problem at the BS. We formulate the corresponding optimization problem for the power allocation factor as

$$\begin{aligned}\mathbf{P}_{\rho}: \underset{\boldsymbol{\rho}}{\text{maximize}} \;& \sum\nolimits_{k\in\mathcal{K}_0} a_k \log_2(1+\gamma_k), \\ \text{s.t.} \;& C_1: \gamma_k \geq \gamma_k^{\mathrm{th}}, \quad \text{for} \quad k \in \mathcal{K}_0, \\ & C_2. \end{aligned} \quad (14)$$

We note that $\mathbf{P}_{\mathrm{w}}$ and $\mathbf{P1}_{\rho}$ are not convex because of the non-convexity of the corresponding objective functions and the constraints. We employ the AO technique and alternately maximize $\mathbf{P}_{\mathrm{w}}$ and $\mathbf{P1}_{\rho}$ until the WSR objective converges.

1) Transmit Beamforming: We introduce β_k to replace the SINR terms in C_1 (13) such that $\beta_k \leq \gamma_k$, $\mathbf{P}_{\mathrm{w}}$ can be reformulated to a standard FP problem [16] as

$$\begin{aligned}\mathbf{P}_{\mathrm{w1}}: \underset{\mathbf{w},\boldsymbol{\beta}}{\text{maximize}} \;& \sum\nolimits_{k\in\mathcal{K}_0} a_k \log_2(1+\beta_k), \\ \text{s.t.} \;& C_1': \gamma_k^{\mathrm{th}} \leq \beta_k \leq \frac{A_k(\mathbf{w})}{B_k(\mathbf{w})}, \text{ for } k \in \mathcal{K}_0, \\ & C_3 - C_5, \end{aligned} \quad (15)$$

where $\boldsymbol{\beta} = [\beta_0, \ldots, \beta_K]^{\mathrm{T}}$. Here, $A_k(x)$ and $B_k(x)$ are the numerator and denominator of the k-th SINR term as functions $x = \mathbf{w}$. We note that, per (7), to meet the minimum condition of $\gamma_k, k \in \mathcal{K}$, we ensure that both γ_k^k and $\gamma_i^k (\forall i < k)$ satisfy the SINR threshold requirement. Next, $\mathbf{P}_{\mathrm{w1}}$ can be seen as a two-part optimization problem: (i) an outer optimization over $\mathbf{w}$ with fixed $\boldsymbol{\beta}$ and (ii) an inner optimization over $\boldsymbol{\beta}$ with fixed $\mathbf{w}$. We give the inner optimization problem as

$$\begin{aligned}\mathbf{P}_{\mathrm{w2}}: \underset{\boldsymbol{\beta}}{\text{maximize}} \;& \sum\nolimits_{k\in\mathcal{K}_0} a_k \log_2(1+\beta_k), \\ \text{s.t.} \;& C_1': \gamma_k^{\mathrm{th}} \leq \beta_k \leq \frac{A_k(\mathbf{w})}{B_k(\mathbf{w})}, \text{ for } k \in \mathcal{K}_0. \end{aligned} \quad (16)$$

The inner optimization problem in (16) is convex in $\boldsymbol{\beta}$ and holds strong duality [16]. Hence, the trivial solution to it is that β_k satisfies C_1' with equality, i.e., $\beta_k^o = A_k(\mathbf{w})/B_k(\mathbf{w})$. To tackle the logarithm in the objective function of $\mathbf{P}_{\mathrm{w2}}$, we apply the Lagrangian dual transform [16], and the corresponding Lagrangian function is given as

$$L(\boldsymbol{\beta}, \boldsymbol{\lambda}) = \sum_{k\in\mathcal{K}_0} a_k \log_2(1+\beta_k) - \sum_{k\in\mathcal{K}_0} \lambda_k \left(\beta_k - \frac{A_k(\mathbf{w})}{B_k(\mathbf{w})}\right), \quad (17)$$

where $\boldsymbol{\lambda} = [\lambda_0, \ldots, \lambda_K]^{\mathrm{T}}$ is the dual variable vector introduced for each inequality constraint in C_1' (16). From the strong duality, we can equivalently reformulate $\mathbf{P}_{\mathrm{w2}}$ to a dual problem as

$$\mathbf{P}_{\mathrm{w3}}: \underset{\boldsymbol{\lambda}\succeq 0}{\text{minimize}} \quad \underset{\boldsymbol{\beta}}{\text{maximize}} \quad L(\boldsymbol{\beta}, \boldsymbol{\lambda}). \quad (18)$$

By evaluating the first-order condition $\partial L(\boldsymbol{\beta}, \boldsymbol{\lambda})/\partial \beta_k, k \in \mathcal{K}_0$ and using the trivial solution to the inner optimization problem, we obtain the optimal solution of λ_k as

$$\lambda_k^o = \frac{a_k B_k(\mathbf{w})}{A_k(\mathbf{w}) + B_k(\mathbf{w})}, \quad \text{for} \quad k \in \mathcal{K}_0. \quad (19)$$

We note that $\lambda_k \geq 0$ is automatically satisfied in this case. From (16) and (19), we reformulate the inner optimization as

$$\mathbf{P}_{\mathrm{w4}}: \underset{\boldsymbol{\beta}}{\text{maximize}} \quad L(\boldsymbol{\beta}, \boldsymbol{\lambda}^o). \quad (20)$$

Furthermore, we can prove that when coupled with the outer optimization over $\mathbf{w}$ and after several mathematical interpretations, the solution to $\mathbf{P}_{\mathrm{w4}}$ also satisfies $\mathbf{P}_{\mathrm{w1}}$ [16]. Additionally, the beamforming vector, $\mathbf{w}$, is obtained by solving the feasibility problem over $\mathbf{w}$ for fixed $\boldsymbol{\beta}$ (15). The detailed steps of the proposed solutions are outlined in Algorithm 1.

Algorithm 1 : WSRMax for transmit beamforming.

Initialization: Initialize $\mathbf{w}$ to a feasible value.
Repeat
Step 1: Update $\boldsymbol{\lambda}$ by (19).
Step 2: Update $\boldsymbol{\beta}$ by solving $\mathbf{P}_{\mathrm{w4}}$ in (20).
Step 3: Update $\mathbf{w}$ by solving feasibility problem over $\mathbf{w}$ for fixed $\boldsymbol{\beta}$ (15).
Until the value of the objective function converges.
Output: The optimal beamforming vector $\mathbf{w}^o$.

2) Power Allocation: Following a similar approach to $\mathbf{P}_{\mathrm{w}}$, we introduce a new variable θ_k for replacing each SINR term in the objective function (14), and $\mathbf{P1}_{\rho}$ is reformulated as

$$\begin{aligned}\mathbf{P}_{\rho 1}: \underset{\boldsymbol{\rho},\boldsymbol{\theta}}{\text{maximize}} \;& \sum\nolimits_{k\in\mathcal{K}_0} a_k \log_2(1+\theta_k), \\ \text{s.t.} \;& C''_1: \gamma_k^{\mathrm{th}} \leq \theta_k \leq \frac{A_k(\boldsymbol{\rho})}{B_k(\boldsymbol{\rho})}, \text{ for } k \in \mathcal{K}_0, \\ & C_2. \end{aligned} \quad (21)$$

where $\boldsymbol{\theta} = [\theta_0, \ldots, \theta_K]^{\mathrm{T}}$. Similar to $\mathbf{P}_{\mathrm{w1}}$, $\mathbf{P}_{\rho 1}$ is also a two part optimization problem. For a fixed $\boldsymbol{\rho}$, the inner optimization problem is given as

$$\mathbf{P}_{\rho 2}: \underset{\boldsymbol{\theta}}{\text{maximize}} \ \sum\nolimits_{k\in\mathcal{K}_0} a_k \log_2(1+\theta_k), \quad \text{s.t. } C_1'': \gamma_k^{\mathrm{th}} \le \theta_k \le \frac{A_k(\boldsymbol{\rho})}{B_k(\boldsymbol{\rho})}, \ \text{for } k \in \mathcal{K}_0. \quad (22)$$

By introducing a dual variable, y_k, the corresponding Lagrangian function is given as

$$L(\boldsymbol{\theta}, \mathbf{y}) = \sum_{k\in\mathcal{K}_0} a_k \log_2(1+\theta_k) - \sum_{k\in\mathcal{K}_0} y_k \left(\theta_k - \frac{A_k(\boldsymbol{\rho})}{B_k(\boldsymbol{\rho})}\right), \quad (23)$$

where $\mathbf{y} = [y_0, \ldots, y_K]^{\mathrm{T}}$. Due to strong duality, $\mathbf{P}_{\rho 2}$ can be equivalently reformulated as

$$\mathbf{P}_{\rho 3}: \underset{\mathbf{y}\succeq 0}{\text{minimize}} \quad \underset{\boldsymbol{\beta}}{\text{maximize}} \quad L(\boldsymbol{\theta}, \mathbf{y}). \quad (24)$$

Next, we evaluate the first-order condition $\partial L(\boldsymbol{\theta}, \mathbf{y})/\partial \theta_k, k \in \mathcal{K}_0$ to obtain the optimal value of the dual variable y_k as

$$y_k^o = \frac{a_k B_k(\boldsymbol{\rho})}{A_k(\boldsymbol{\rho}) + B_k(\boldsymbol{\rho})}, \quad \text{for} \quad k \in \mathcal{K}_0. \quad (25)$$

Hence, $\mathbf{P}_{\rho 2}$ is equivalent to

$$\mathbf{P}_{\rho 4}: \underset{\boldsymbol{\theta}}{\text{maximize}} \quad L(\boldsymbol{\theta}, \mathbf{y}^o). \quad (26)$$

Algorithm 2 shows the proposed approach for solving $\mathbf{P}_{\rho}(14)$.

Algorithm 2 : WSRMax for power allocation.

Initialization: Initialize $\boldsymbol{\rho}$ to a feasible value.
Repeat
Step 1: Update $\mathbf{y}$ by (25).
Step 2: Update $\boldsymbol{\theta}$ by solving $\mathbf{P}_{\rho 4}$ in (26).
Step 3: Update $\boldsymbol{\rho}$ by solving feasibility problem over $\boldsymbol{\rho}$ for fixed $\boldsymbol{\theta}$ (21).
Until the value of the objective function converges.
Output: The optimal power allocation factor $\boldsymbol{\rho}^o$.

Remark 1. *Algorithms 1 and 2 outline the proposed approaches for solving* $\mathbf{w}$ *by fixing* $\boldsymbol{\rho}$ *and for solving* $\boldsymbol{\rho}$ *by fixing* $\mathbf{w}$ *after the original problem,* $\mathbf{P}$*, is separated into two sub-problems. We begin by quantifying* U_k*'s SINR, and the tag as we initialize* $\mathbf{w}$ *and* $\boldsymbol{\rho}$ *to feasible values. Then, better solutions for* $\mathbf{w}$ *and* $\boldsymbol{\rho}$ *are updated in each iteration. The procedure is repeated until there is no further improvement. At this point, it is terminated by a condition such that the increment of the normalized objective function is smaller than* $\epsilon = 10^{-3}$.

A. Computational Complexity

The proposed algorithm has multiple stages. The outer loop comprises two sub-problems for optimizing $\mathbf{w}$ (Algorithm 1) and $\boldsymbol{\rho}$ (Algorithm 2). The main complexity of these two lies in step 3. As CVX Matlab applies an SDPT3 solver to handle these optimization problems, the computational complexities are $\mathcal{O}((K+1)^3 M^3)$ and $\mathcal{O}((K+1)^3)$, respectively [17]. Hence, the proposed solution for WSRMax has a total complexity of $\mathcal{O}(I_o^W (I_w (K+1)^3 M^3 + I_\rho (K+1)^3))$, where I_w, I_ρ, and I_o^W are the iteration numbers of Algorithm 1, Algorithm 2, and the overall algorithm (outer loop), respectively. Note that the overall algorithm converges in less than 4 iterations regardless of the BS transmit power.

V. Simulation Results

Herein, we provide simulation examples to evaluate the benefits/harms of symbiosis. We adopt the 3GPP UMi model to model ζ_a (1) with $f_c = 3\,\mathrm{GHz}$ operating frequency [18, Table B.1.2.1]. The AWGN variance, σ^2, is modeled as $\sigma^2 = 10\log_{10}(N_0 B N_f)$ dBm, where $N_0 = -174\,\mathrm{dBm/Hz}$, $B = 10\,\mathrm{MHz}$ is the bandwidth, and $N_f = 10\,\mathrm{dB}$ is the noise figure. Moreover, $M = 32$, $a_k = 1/(K+1), k \in \mathcal{K}_0$, $p_b = -20\,\mathrm{dBm}$, and $\eta_b = 0.6$.

To evaluate the performance, we also consider a non-symbiotic NOMA network without the tag and solve the WSRMax problem. Herein, we consider $K = 2$ primary NOMA users and investigate the rate performances of the primary users and the tag, and the EH constraint at the tag through the proposed solutions for the WSRMax problem (Section IV). We consider the rate requirements as $R_0^{\mathrm{th}} = \log_2(1+p_t/100)$, $R_1^{\mathrm{th}} = \log_2(1+p_t)$, and $R_2^{\mathrm{th}} = \log_2(1+p_t/10)$.

To benchmark our algorithm, we also consider weighted maximum ratio transmission (MRT) and random beamforming designs. For the latter, a complex Gaussian random vector is selected to satisfy the NOMA constraint (3). It does not require CSI, and the beam can be focused in any direction, resulting in poor performance. Weighted MRT is designed as $0.5\mathbf{h}_1/\|\mathbf{h}_1\| + 0.5\mathbf{h}_2/\|\mathbf{h}_2\|$. It directs the beam toward the primary users and thus needs accurate CSI. For both designs, we set $\rho_1 = 0.3$ to satisfy C_2 (11). We assume $d_f = 5\,\mathrm{m}$, $d_{h_1} = d_{h_2} = 12\,\mathrm{m}$, $d_{q_1} = 8\,\mathrm{m}$, $d_{q_2} = 10\,\mathrm{m}$, and $\alpha = 0.6$.

Fig. 2 investigates the symbiosis benefits to the tag and the effects of the tag's reflection coefficient to the added benefits. It depicts the trade-off between the harvested energy and the tag rate as a function of the α with different transmit beamforming vectors, for $p_t = 20\,\mathrm{dBm}$. As α approaches 1, the tag reflects most of the received power and achieves the maximum rate. However, this is not a feasible operating point for a passive tag, which must harvest energy. When α approaches 0, the tag harvests most of the received power, and the rate becomes infinitesimal since the tag does not reflect any signal. Hence, for given α, the amount of achieved rate and harvested power traverse this trade-off curve. Because the tag must harvest a minimum power, we need $\alpha \in (0,1)$. We also observe that, unlike random and MRT beamforming, our beamforming design significantly enhances the symbiotic benefits to the tag.

To investigate the overall benefits of symbiosis and the advantages of NOMA, Fig. 3 and Fig. 4 respectively show the rates of the user and the tags under different BS beamforming designs. In Fig. 4, R_0^{lb} is the lower bound rate obtained through (12) and R_0 (9) is the actual rate of the tag.

Fig. 3 shows that without our designs, the symbiotic gains are negligible. For example, with random beamforming, the user rates are the lowest. Also, weighted MRT beamforming is computed without symbiotic goals in mind. It merely shapes

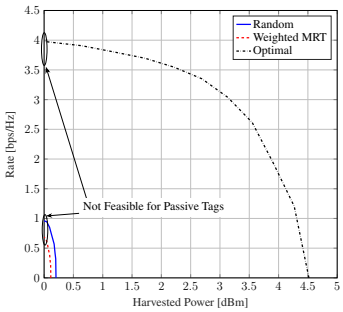

Fig. 2: Tag's harvested power and rate trade-off.

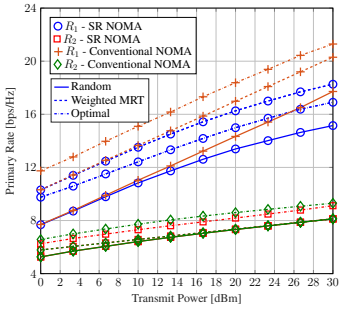

Fig. 3: The rate of the users versus transmit power.

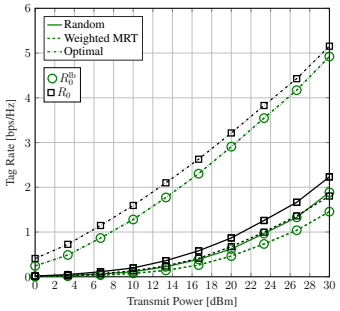

Fig. 4: Tag rate versus transmit power.

the beam towards the users (ignoring the tag). Then U_2 achieves a low rate. However, U_1 achieves the highest rate because it performs SIC and cancels out the signal of U_2. On the other hand, with our designs, the two users achieve acceptable rates, exceeding the threshold rates, while also enhancing the harvested power and the rate performance of the tag (Fig. 2 and Fig. 4). As observed, the rate performance of the tag significantly improves, and it achieves the highest rate while preserving the performance of the NOMA users.

If we compare (a) the SR network and (b) the equivalent NOMA system without the tag, the two users achieve the highest rates for (b) with proposed beamforming designs. Network (b) can also work with reduced transmit BS powers for certain rates of users. For example, in (a), for $13.32\,\text{bps/Hz}$ and $7.6\,\text{bps/Hz}$ and $2.1\,\text{bps/Hz}$ for U_1 and U_2 and the tag (Fig. 4), respectively, BS requires $13.33\,\text{dBm}$. However, in (b), the required power decreases by $\sim$6 dBm to achieve those rates for U_1 and U_2 (U_1 achieves $13.32\,\text{bps/Hz}$ at $p_t = 6.27\,\text{dBm}$ and U_2 achieves $7.6\,\text{bps/Hz}$ at $p_t = 8.33\,\text{dBm}$). Thus, symbiotic gains are not without costs. In (b), the user rates can be supported without considering the tag. In (a), the BS must compensate for the deep fading of the tag channels and ensure that the tag will harvest enough. Nonetheless, our algorithm ensures symbiosis has overall benefits as the performance requirements of both primary users and the tag can be satisfied. Moreover, the SR system (a) has a slight rate loss compared to the network (b), $\sim$0.9 bps/Hz at $p_t = 16\,\text{dBm}$.

VI. Conclusion

In this paper, we investigated the symbiosis between a primary NOMA network and an AmBC tag. We designed the optimal BS beamformer and power allocation to maximize the WSR of the primary and tag rates under the users' and the tag's minimum rate requirements and the tag EH constraint. Because the problem is non-convex, we developed solution algorithms based on AO and FP techniques. The resulting BS designs achieve significant performance gains while simultaneously satisfying the rate requirements, with no tag modifications.

References

[1] R. Long, Y.-C. Liang, H. Guo, G. Yang, and R. Zhang, "Symbiotic radio: A new communication paradigm for passive internet of things," *IEEE Internet Things J.*, vol. 7, no. 2, pp. 1350–1363, 2020.

[2] D. Galappaththige, F. Rezaei, C. Tellambura, and S. Herath, "Link budget analysis for backscatter-based passive IoT," *IEEE Access*, vol. 10, pp. 128 890–128 922, Dec. 2022.

[3] F. Rezaei, D. Galappaththige, C. Tellambura, and S. Herath, "Coding techniques for backscatter communications - A contemporary survey," *IEEE Commun. Surveys Tuts.*, pp. 1020–1058, 2th Quart. 2023.

[4] T. Wu, M. Jiang, Q. Zhang, Q. Li, and J. Qin, "Beamforming design in multiple-input-multiple-output symbiotic radio backscatter systems," *IEEE Commun. Lett.*, vol. 25, no. 6, pp. 1949–1953, Jun. 2021.

[5] Z. Ding *et al.*, "A survey on non-orthogonal multiple access for 5G networks: Research challenges and future trends," *IEEE J. Sel. Areas Commun.*, vol. 35, no. 10, pp. 2181–2195, Oct. 2017.

[6] Y. Zhuang, X. Li, H. Ji, and H. Zhang, "Exploiting intelligent reflecting surface for energy efficiency in ambient backscatter communication-enabled NOMA networks," *IEEE Trans. Green Commun. Netw.*, vol. 6, no. 1, pp. 163–174, Mar. 2022.

[7] W. U. Khan, X. Li, M. Zeng, and O. A. Dobre, "Backscatter-enabled NOMA for future 6G systems: A new optimization framework under imperfect SIC," *IEEE Commun. Lett.*, vol. 25, no. 5, pp. 1669–1672, May 2021.

[8] Y. Xu, Z. Qin, G. Gui, H. Gacanin, H. Sari, and F. Adachi, "Energy efficiency maximization in NOMA enabled backscatter communications with QoS guarantee," *IEEE Wireless Commun. Lett.*, vol. 10, no. 2, pp. 353–357, Feb. 2021.

[9] M. Ahmed, W. U. Khan, A. Ihsan, X. Li, J. Li, and T. A. Tsiftsis, "Backscatter sensors communication for 6G low-powered NOMA-enabled IoT networks under imperfect SIC," *IEEE Syst. J.*, Dec. 2022.

[10] W. U. Khan, M. A. Javed, T. N. Nguyen, S. Khan, and B. M. Elhalawany, "Energy-efficient resource allocation for 6G backscatter-enabled NOMA IoV networks," *IEEE Trans. Intell. Transp. Syst.*, pp. 1–11, Jul. 2022.

[11] W. U. Khan, F. Jameel, N. Kumar, R. Jäntti, and M. Guizani, "Backscatter-enabled efficient V2X communication with non-orthogonal multiple access," *IEEE Trans. Veh. Technol.*, vol. 70, no. 2, pp. 1724–1735, Feb. 2021.

[12] W. Chen, H. Ding, S. Wang, D. B. da Costa, F. Gong, and P. H. J. Nardelli, "Ambient backscatter communications over NOMA downlink channels," *China Commun.*, vol. 17, no. 6, pp. 80–100, Jun. 2020.

[13] F. Rezaei, D. Galappaththige, C. Tellambura, and A. Maaref, "Time-spread pilot-based channel estimation for backscatter networks," *arXiv preprint arXiv:2305.17248*, 2023.

[14] F. Rezaei, C. Tellambura, A. A. Tadaion, and A. R. Heidarpour, "Rate analysis of cell-free massive MIMO-NOMA with three linear precoders," *IEEE Trans. Commun.*, vol. 68, no. 6, pp. 3480–3494, Jun. 2020.

[15] Q. Zhang, S. Jin, K.-K. Wong, H. Zhu, and M. Matthaiou, "Power scaling of uplink massive MIMO systems with arbitrary-rank channel means," *IEEE J. Sel. Topics Signal Process.*, vol. 8, no. 5, pp. 966–981, May 2014.

[16] K. Shen and W. Yu, "Fractional programming for communication systems—part i: Power control and beamforming," *IEEE Trans. Signal Process.*, vol. 66, no. 10, pp. 2616–2630, May 2018.

[17] A. Ben-Tal and A. S. Nemirovskiaei, *Lectures on Modern Convex Optimization: Analysis, Algorithms, and Engineering Applications*. USA: Society for Industrial and Applied Mathematics, 2001.

[18] "3GPP TR 36.814, further advancements for E-UTRA physical layer aspects, V.9.0.0 Rel. 9," Mar. 2010. Available Online: https://portal.3gpp.org/desktopmodules/Specifications/SpecificationDetails.aspx?specificationId=2493.